ELSEVIER

Chemical Engineering Journal 73 (1999) 173–190

Chemical Engineering Journal

Multi-stage flash desalination: present and future outlook

Hisham T. El-Dessouky*, Hisham M. Ettouney, Yousef Al-Roumi

Department of Chemical Engineering, Kuwait University, PO Box 5969, Safat 13060, Kuwait

Received 31 March 1998; received in revised form 31 January 1999; accepted 8 February 1999

Abstract

Multi-stage flash desalination (MSF) is currently the workhorse of the desalination industry with a market share close to 60% of the total world production capacity. As the turning point of the new millennium nears, the process faces many challenges dictated by industrial demands and public needs. The conservative nature of the desalination owner, as well as the strategic characteristics of the product, makes the MSF process favored over other competitive thermal desalination methods. In addition, the process has several merits, which include a large production capacity, proven reliability and well-developed construction and operation experience. This study offers an overview of the present and future developments in the MSF process, which aims to reduce the production cost. Special attention is given to the process fundamentals, which are the key elements for any serious and physically sound development of the MSF process. Also, a summary of the novel (MSF-M) configuration is given, which has recently been proposed by the authors. The process is based on the modification of operational MSF plants as well as the concept of once-through MSF. The modification involves removal of the heat rejection section and the addition of a mixing tank for the feed stream and the unevaporated brine recycle. This eliminates the amount of energy rejected in the cooling seawater stream and reduces the amount of energy rejected in the brine blowdown stream. Analysis of the MSF-M process shows an increase in the thermal performance ratio by a factor of 2–3 over conventional MSF.

Keywords: Water desalination; Single-stage flashing; Multi-stage flashing; Brine recycle; Modeling and simulation

1. Introduction

Global resources of freshwater are scarce, unevenly distributed and, in many cases, may require some form of treatment and handling. These limited resources have resulted in water shortages in 88 developing countries across the world containing 50% of the world's population [1]. Water supplies in these countries cannot meet urban and industrial development needs as well as associated changes in lifestyle. Moreover, common use of poor water in developing countries causes 80–90% of all diseases and 30% of all deaths. Even in industrial countries, long dry seasons and limited rainfall force governments, states, and municipalities to adopt severe water restriction programs that affect the population at large [2]. Such situations are reported on a frequent basis in several countries around the globe. The current water shortage extends to include underground water supplies, previously considered to be an unlimited resource in many countries. In this regard, several cases have been reported of well failure, decline of the water table and seawater intrusion into freshwater aquifers. This situation has forced many countries, industrial and developing, to adopt active and efficient programs for the reclamation of industrial and municipal wastewater. Reclaimed industrial wastewater is recycled a number of times through the process, before being bound into the final product, rejected to a receiving body of water, injected in underground aquifers or lost as water vapor. On the other hand, municipal wastewater is treated before being used for crop irrigation or aquifer injection.

In many arid zones, coastal or inland, desalination of seawater or brackish water may be the only solution for a supply of freshwater. Due to the strategic nature of the product, many countries favor to the adoption of the relatively expensive desalination process, which has been proved to provide a sustainable source. The adoption of the desalination process by the Gulf States, as well as by a number of industrial countries, has resulted in rapid progress in the industry since its inception in the 1950s. Since then, the number of operating units has increased from a handful to more than 11 000 units in 1996 [3]. This increase in the production volume has been associated with a decrease in the power consumption from 100–250 kW per 1000 gallons in 1955 to 15–40 kW per 1000 gallons. Similar progress has

*Corresponding author. E-mail: eldessouky@kuc01.kuniv.edu.kw

1385-8947/99/$ – see front matter
PII: S1385-8947(99)00035-2

occurred in the MSF process, where the unit capacity has increased from a small capacity of 0.5 mgd during the 1950s and 1960s to a current unit capacity varying from 7 to 12.5 mgd [4].

Despite this progress, the desalination process remains expensive and inaccessible to many countries in the world. The limited means of many countries cannot meet the required process capital and operating expenses. Bednarski et al. [5] reported the current water production cost of the multi-stage flash desalination (MSF), RO and multiple effect evaporation (MEE) processes. For the MSF process, with a 6 mgd plant, the unit cost is \$0.8 m^{-3}. This compares favorably with RO technology, with a cost range of \$0.72–0.93 m^{-3}, which is highly dependent on the treatment cost of feed water. Although a lower unit cost is reported for the MEE process, with a value of \$0.45 m^{-3}, the adoption of this method by the desalination industry is found on a very limited scale. The lower unit cost in the MEE process is primarily caused by the higher thermal performance ratio. These production values remain higher than the cost of pipeline transportation of freshwater from a distant source to the supply point. For example, in Virginia Beach, USA, the transportation of freshwater from Lake Gaston, which is located 76 miles away, is less expensive than the production cost of a desalination plant [6]. That study showed that the desalination unit cost was \$1.22 m^{-3} and the transportation unit cost was \$0.74 m^{-3}.

In spite of the development and progress in the MSF process, especially the large increase in capacity and reduction in power consumption, the performance ratio has remained at a value of eight for more than two decades. This value is 30–70% lower than the MEE system or MEE combined with vapor compression heat pumps [7–12]. The development of these processes is focused on the improvement of the thermal performance ratio or specific power consumption. Existing MEE units combined with thermal vapor compression give design values of 12–16 for the thermal performance ratio. The process is limited to low temperature operation, which requires a large heat transfer area in comparison with the MSF process. MEE design and analysis at higher temperatures show a drastic reduction in the specific heat transfer area to values similar to or lower than that of the MSF process [12]. Field data on the MEE system by de Gunzbourg and Larger [13] show consistent results, where an existing MEE system is reported to have thermal performance ratios of 12 in stand-alone mode, 16 when combined with thermal vapor compression, and 21 when combined with lithium bromide/water absorption heat pump.

Field data for single effect evaporation and MEE combined with mechanical vapor compression show competitive power consumption against the RO process [14]. Moreover, the process has the basic operational features of other thermal processes, with a high plant factor, simple feed pretreatment and low capital. The drawbacks of the process are primarily caused by limitations on the compressor range, which limits operation to low temperatures. This requires a large heat transfer area for the evaporator/condenser tubes. In addition, the process uses expensive electrical energy. Despite the attractive features of single effect evaporation and MEE systems, and their higher thermal performance ratio, especially when combined with heat pumps [15–18], only a limited number of industrial units are found, primarily because of a lack of construction and operation experience.

The MSF process has many attractive features, which distinguish it from other desalination configurations. Since its establishment in the late 1950s, enormous field experience has been accumulating in process technology, design procedure, construction practice and operation. This has resulted in the development of simple and reliable operational procedures. In addition, the development has addressed and solved various operational problems, including scale formation, foaming, fouling and corrosion [19–22]. Experience gained in the operation and design of MSF plants has led to the use of inexpensive construction materials capable of withstanding harsh conditions at high salinity [23–25]. The MSF system does not include moving parts, other than conventional pumps. Construction of the MSF plants is simple and involves a small number of connection tubes, which limits leakage problems and simplifies maintenance work.

In the light of the above, we strongly believe that the MSF system will remain the main desalination process, especially in the Middle East. This is due to the following:

1. the conservative nature of the desalination owner;
2. the product is a strategic life-supporting element;
3. extensive experience in construction and operation;
4. process reliability;
5. limited experience, small database, and unknown risks with new technologies.

It should be stressed that the market share of MSF in the desalination industry will remain at its current level as long as significant milestones are achieved at a similar rate to that in the past four decades. This motivated the present study, which focuses on two elements essential for process development:

1. The fundamentals of the MSF process, which are the key elements in proper process design, rating, control, optimization and development;
2. Addressing the problem of the low thermal performance ratio of MSF in comparison with other thermal desalination processes; this is performed by developing the brine-mixing MSF configuration, MSF-M.

As discussed later, adoption of the second element, which is based on the modification of existing MSF units to improve their thermal performance, might be a more viable proposal than the construction of large-scale MSF units, which are inherently different in makeup and operation than conventional MSF units, or the replacement with MEE

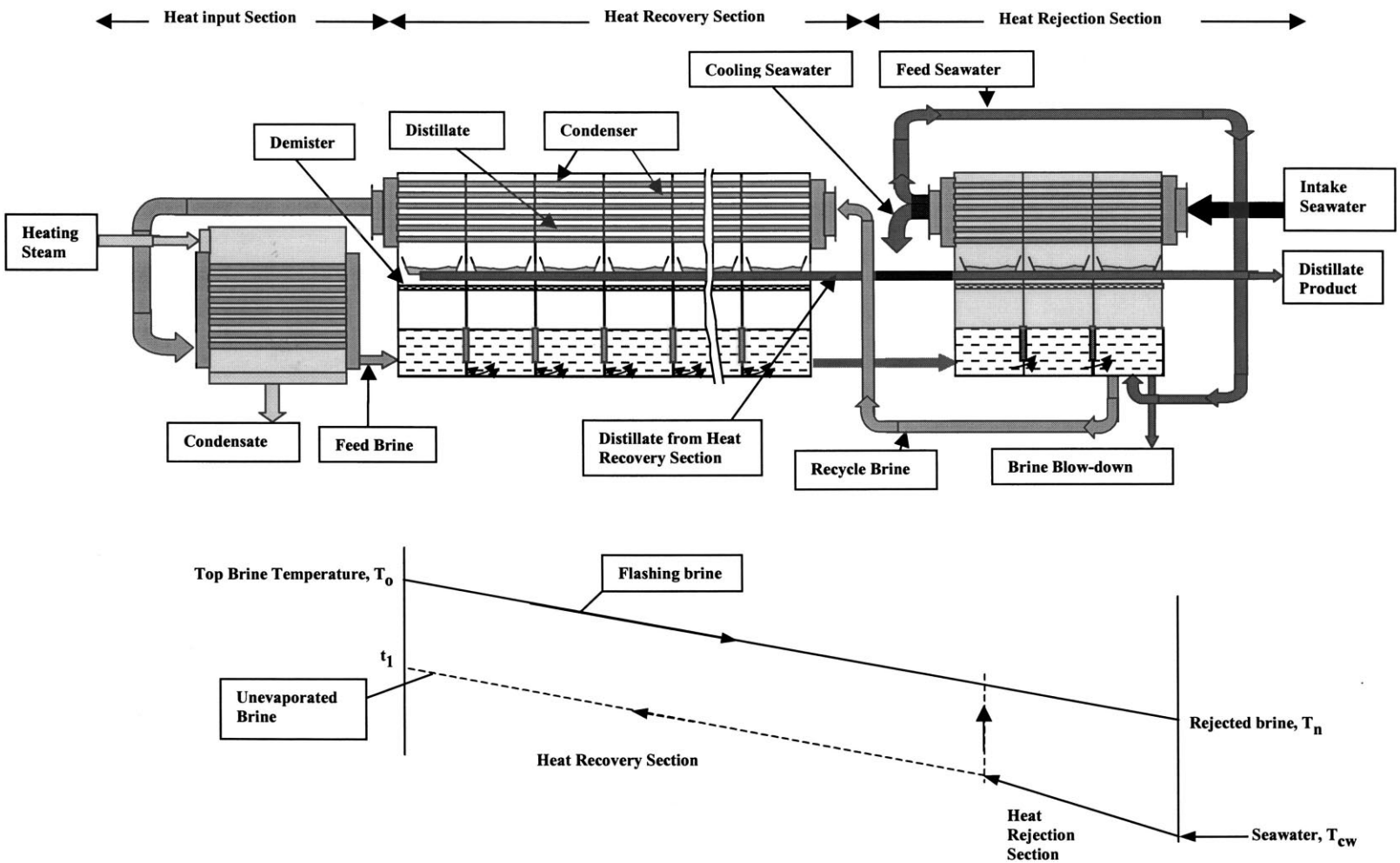

Fig. 1. Multi-stage flash desalination process and temperature profiles.

systems. The following sections include process description, fundamentals of MSF, performance analysis of MSF-M and conclusions.

2. Description of the MSF process

Fig. 1 shows a schematic diagram of the MSF system. The system involves six main streams: intake seawater, rejected cooling seawater, distillate product, rejected brine, brine recycle and heating steam. The system contains flashing stages, a brine heater, pumping units, venting system, and a cooling water control loop. The flashing stages are divided into two sections: heat recovery and heat rejection. The number of flashing stages in the heat rejection section is commonly limited to three. On the other hand, the number of flashing stages in the heat recovery section varies between 21 and 40. The intake seawater is introduced into the inside of the preheater/condenser tubes of the last flashing stage in the heat rejection section. Similarly, the brine recycle stream is introduced into the inside of the preheater/condenser tubes of the last flashing stage in the heat recovery section. The flashing brine flows counter to the brine recycle from the first to the last flashing stage.

The saturated heating steam with a temperature range of 97–117°C drives the flashing process. The heating steam flows on the outside of the brine heater tubes and the brine stream flows on the inside of the tubes. As the heating steam condenses, the brine stream gains the latent heat of condensation and its temperature reaches the desired top brine temperature. This parameter, together with the flashing temperature in the last stage, defines the total flashing range.

The hot brine enters the first flashing stage, where a small amount of product vapor is formed. The flashing process reduces the temperature of the unevaporated brine. The temperature reduction across the flashing stages is associated with a drop in the stage pressure, where the highest stage pressure is found in the first stage after the brine heater and the lowest pressure is that of the last stage. The pressure drop across the stages allows for brine flow without the use of interstage pumping units.

In each stage, the flashed off vapor flows through the demister, which removes entrained droplets of unevaporated brine. The vapor then condenses on the outside surface of the preheater/condenser tubes. The condensed vapor collects over the distillate trays across the flashing stages to form the final product water, which is withdrawn from the last flashing stage. The condensation process releases the vapor latent heat, which is used to preheat the brine recycle stream in the heat recovery section. The same process takes place in the preheater/condenser tubes in the heat rejection section. This results in an increase in the seawater temperature to a higher value, equal to the temperature of the flashing brine, in the last stage of the heat rejection section. The intake seawater stream leaves the heat rejection section, where it splits into two streams. The first stream is the cooling seawater stream, which is rejected back to the sea, and the second is the feed seawater stream, which is mixed in the brine pool in the last flashing stage in the heat rejection section. Prior to the mixing location of the feed seawater stream, the rejected brine stream is withdrawn from the brine pool. On the other hand, the brine recycle is withdrawn from a location after the mixing point. The brine blowdown is rejected to the sea and the brine recycle is introduced to the last stage in the heat recovery section.

Additional units in the desalination plant include pretreatment of the feed and intake seawater streams. Treatment of the intake seawater is limited to simple screening and filtration. On the other hand, treatment of the feed seawater is more extensive and includes deaeration and addition of antiscalant and foaming inhibitors. Other basic units in the system include pumping units for the feed seawater, brine recycle and brine blowdown.

The release of non-condensable gases occurs simultaneously with the flashing process. The presence of non-condensable gases reduces the efficiency of the vapor condensation process. This is caused by the low thermal conductivity of the non-condensable gases, which act as an insulating layer around the preheater/condenser tubes. In addition, the presence of non-condensable gases reduces the saturation pressure of the flashing vapor, which results in a lower condensation temperature. Consequently, the driving force for condensation is reduced and so is the overall thermal efficiency of the process. To prevent the accumulation of non-condensable gases and their harmful effects on the condensation process, gas venting units are used to withdraw the non-condensable gases from a number of flashing stages. Steam jet ejectors are adopted to generate sufficient vacuum to withdraw the gases from collection points near the preheater/condenser tubes. The selection of these locations is necessary to minimize undesirable losses of the flashing vapor.

3. Fundamentals of MSF

Understanding the complex nature of the MSF layout and the functions and relations of various process elements is essential for successful system analysis, optimization, operation and control. Also, this is important in the development and design of novel and more efficient desalination processes. To achieve the desired goal, a number of questions are first posed concerning system configuration:

1. the maximum or minimum limits on the total number of flashing stages;
2. the limiting number of flashing stages in the heat rejection and recovery sections;
3. the function of the flashing stages in the heat recovery and rejection sections;
4. the maximum and minimum top brine temperatures;
5. the functions of the brine recycle, cooling seawater and rejected brine.

The following analysis dissects the process flow diagram. This involves stepwise analysis and starts with the simplest configuration, which is the single-stage flashing system. The analysis continues through subsequent configurations, improving on the operational drawbacks of the previous system. As discussed later, reaching the configuration of conventional MSF is made through four development steps, which include the following:

1. the single-stage flashing unit;
2. the once-through multi-stage flash system, MSF-OT;
3. the brine-mixing multi-stage flash system, MSF-M;
4. the conventional MSF system.

Analytical and non-iterative mathematical models are used to analyze the above systems. Analytical models of the MSF process are efficient, with reasonable accuracy to determine the major features of the system [26]. However, it should be stressed that acquiring detailed and more accurate design and rating data necessitates the use of rigorous numerical models (see for example, the studies by Omar [27] Helal et al. [28] Montagna [29] Hussain et al. [30] Rosso et al. [31] El-Dessouky et al. [32] and El-Dessouky and Bingulac [33].

To adopt the analytical solution method, the following assumptions are invoked:

1. linear profiles for the temperature of the flashing brine stream and the feed seawater flowing inside the preheater condenser tubes;
2. the specific heat at constant pressure, C_p, for all liquid streams, brine, distillate, and seawater, is constant with a value of 4.18 kJ $kg^{-1}{}^{\circ}C^{-1}$;
3. the latent heat for vaporization in the multi-stage system is constant and is evaluated at the average temperature for the flashing brine;
4. the overall heat transfer coefficient in the brine heater and the preheater/condenser units is constant and equal to 2 kW $m^{-2}{}^{\circ}C^{-1}$;
5. the thermodynamic losses are constant in all stages and equal to an average value of 1°C.

These assumptions eliminate the non-linear nature of the model equations, which simplifies the solution procedure. Other assumptions, also common in numerical models, are known to have a negligible effect on the accuracy of the model predictions. These assumptions are:

1. subcooling of the condensate or superheating of the vapor has a negligible effect on the system energy balance, since the latent heat is larger than the sensible heat caused by 1–2°C temperature drop;
2. the power requirements for pumps and auxiliaries are not included in the system analysis;
3. the heat losses to the surroundings are negligible because the system is well insulated and operates at low temperatures;
4. the distillate product is salt free; this assumption is valid since the boiling temperature of water is much lower than that of salt.

The evaluation of the various desalination configurations is based on the following set of parameters:

1. the thermal performance ratio is the mass of product water per unit mass of heating steam, $PR=M_d/M_s$;
2. the specific heat transfer area is the total heat transfer area required per unit mass of distillate product, $sA=A/M_d$;
3. the specific feed flow rate is the ratio of the feed to distillate flow rates, $sM_f=M_f/M_d$;
4. the specific cooling water flow rate is the ratio of the cooling water to distillate flow rates, $sM_{cw}=M_{cw}/M_d$.

These variables are the most important factors controlling the cost of fresh water production.

The following data set is used, unless otherwise specified, to evaluate the performance of various configurations:

1. the top brine temperature, T_o, varies between 90–110°C;
2. the temperature of reject brine, T_n, is 40°C for summer and 32°C for winter;
3. the temperature of the heating steam, T_s, is higher than the top brine temperature by 10°C;
4. the temperature of the intake seawater, T_{cw}, is 30°C for summer and 14.4°C for winter;
5. the salinity of the intake seawater, X_f, is 42 000 ppm, which is typical for the Gulf State countries;
6. the maximum attainable concentration of the rejected brine, X_b, is 70 000 ppm.

The mathematical models used to analyze the MSF fundamentals are given in Appendix B; however, more detailed calculations can be found in the study by El-Dessouky et al.[34].

3.1. Single stage flashing (SSF) unit

The single-stage flashing unit, shown in Fig. 2, contains a brine heater, condenser tubes, and flashing pool. Saturated steam at a flow rate equal to M_s is used to increase the temperature of the feed seawater from t_1 to T_o. The feed seawater, M_f, enters the flashing pool and its temperature drops to T_1. The vapor formed, M_d, is at a temperature, T_{v1}, which is less than T_1 by the thermodynamic losses. The vapor condenses around the condenser tubes and releases its latent heat to the intake seawater stream, $M_{cw}+M_f$. This increases the stream temperature from T_{cw} to t_1. Typical of the SSF system, its performance ratio is always less than unity, or the amount of product distillate water is less than the amount of heating steam. This is given by the relation, $PR=\Delta T_{st}/(\Delta T_{st}+\Delta T_{loss}+TTD_c)$, where the sum of the thermodynamic losses, ΔT_{loss}, and the terminal temperature difference, TTD_c, may vary over a range of 5–10°C. Other

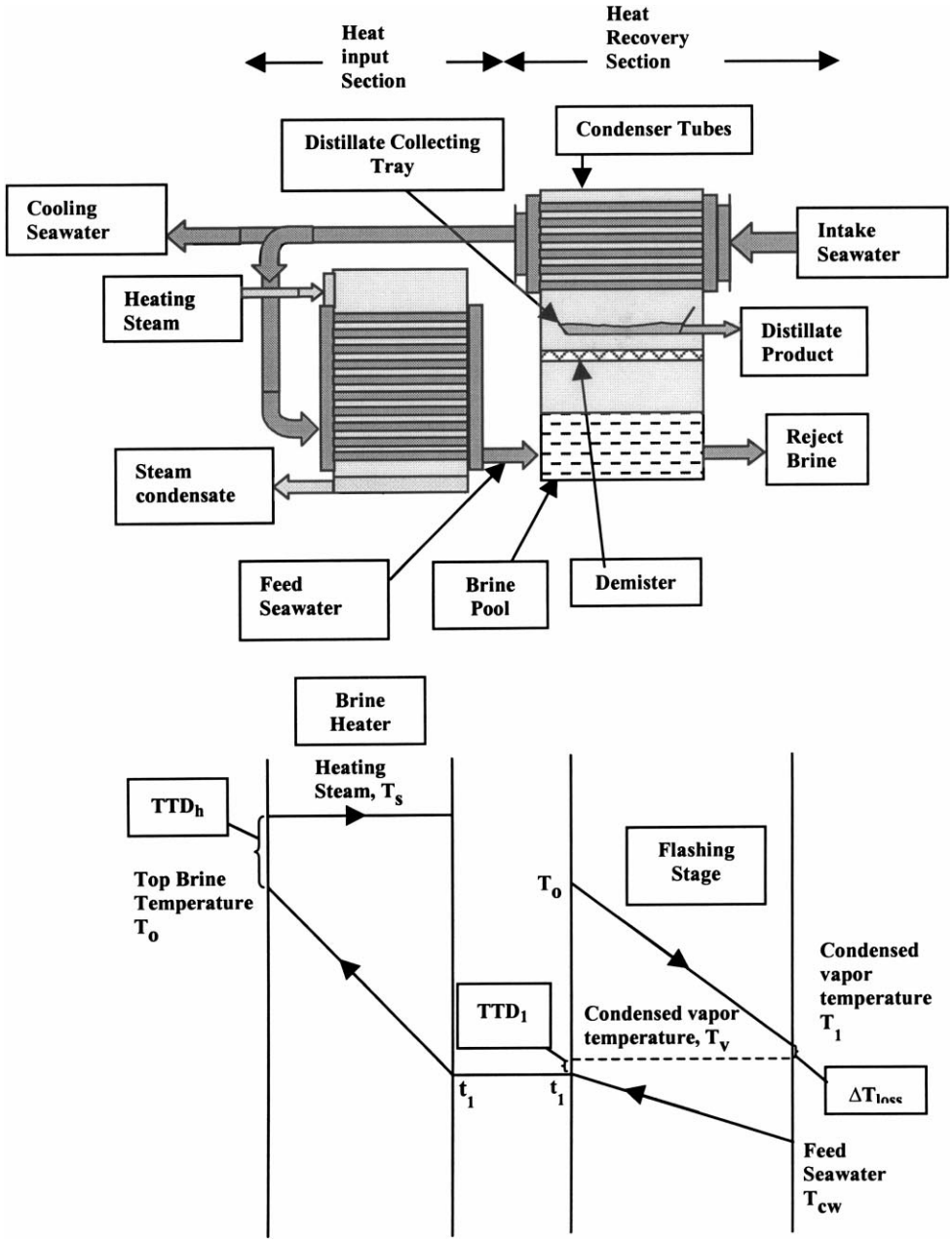

Fig. 2. Single stage flashing unit and temperature profiles.

drawbacks are the large amounts of feed and cooling seawater relative to the amount of product water, where sM_f is 11.54 and sM_{cw} is 103.9. This increases the energy consumption of the pumping unit, as well as the amount of chemical additives and pretreatment.

3.2. Once-through MSF (MSF-OT) unit

The MSF-OT system, (Fig. 3), addresses the low thermal performance ratio and high flow rate of the cooling seawater found in the SSF system. The thermal performance ratio is increased through the use of additional flashing stages and the cooling seawater stream is removed. As shown, the number of stages is increased from 1 to a larger value n, which may vary over a range of 20–45. The process description of the MSF-OT system is similar to that of conventional MSF given in Section 2.

As shown in Table 2 (see later) the thermal performance ratio for the MSF-OT system with 24 stages varies over a low range of 3–4 in winter and 6–7 in summer. The increase in the thermal performance ratio from values below unity found in the SSF unit to higher levels for the MSF-OT unit is caused by a decrease in the flashing range in each stage or by dividing the total flashing range over the number of stages. Also, the thermal performance ratio, as described by the simplified form of Eq. (B.15), PR=$n\Delta T_{st}$/

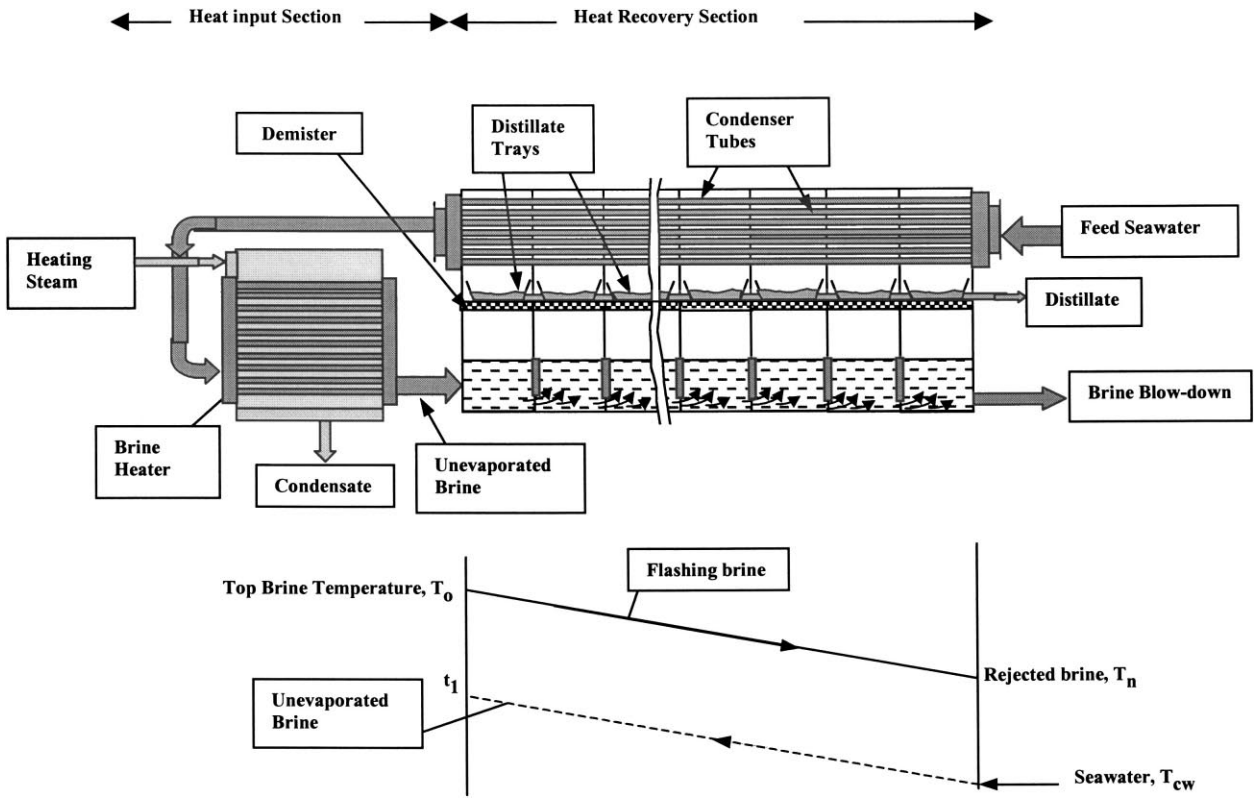

Fig. 3. Once-through MSF desalination plant (MSF-OT) and temperature profiles.

($\Delta T_{st}+\Delta T_{loss}+TTD_c$), clearly shows the effect of increasing the number of stages. On the other hand, the increase in the total specific heat transfer area, sA, to a value of 306.8 $m^2\,kg^{-1}\,s^{-1}$), is caused by the decrease in the temperature difference driving force. A merit feature of the MSF-OT system is the low salinity of the brine reject stream, 46 106.6 ppm, in comparison with the solubility limit of 70 000 ppm. Also, the specific heat transfer area of the brine heater is inversely proportional to the thermal performance ratio. As a result the specific area of the brine heater decreases from 45.2 $m^2\,kg^{-1}\,s^{-1}$ in the SSF unit to 12.69 $m^2\,kg^{-1}\,s^{-1}$) for the MSF-OT system.

Despite the above improvements, the MSF-OT system has a major drawback: the drastic reduction in the system thermal performance ratio during winter operation. This is caused by:

1. the absence of a control mechanism on the seawater temperature, i.e. the heat rejection section in conventional MSF and the mixing tank in MSF-M;
2. the high amount of energy lost in the large rejected brine stream.

The absence of a control mechanism on the temperature of the feed seawater and the associated reduction in the system performance ratio especially during winter operation, limits the use of MSF-OT on an industrial scale. Another system disadvantage is the large flow rate of the feed seawater stream in comparison with the flow rate of the product water stream. This implies a high consumption rate of chemical additives and the use of large treatment units; both factors account for an increase in the capital investment and the operating cost.

3.3. Conventional MSF unit

The results for the MSF system given in Table 2 (see later) show stable operation during winter and summer, with the thermal performance ratio varying over a narrow range of 8–8.56. This stability is a result of the design features of the heat rejection section. During winter operation, part of the reject cooling seawater stream is recycled and mixed with the intake stream. In summer operation, the temperature control of the intake cooling seawater is not necessary, since the temperature difference between the intake seawater, 30°C, and the brine blowdown, 40°C, is 10°C. Therefore, the temperature increase of 10°C for the intake seawater stream takes place in the preheater/condenser units. Another merit of the conventional MSF system is the low flow rate of feed seawater; 2.5 $kg\,s^{-1}$ for each 1 $kg\,s^{-1}$ of product water. As discussed before, this lowers the consumption rate of chemical additives and reduces the size of the pretreatment equipment. The low feed flow rate results in a high salinity of the blowdown brine stream, 70 000 ppm, which implies the efficient use of the feed seawater stream through the generation of the maximum

possible amount of product water. Also, the total specific heat transfer area is low: 287.93 $m^2\ kg^{-1}\ s^{-1}$.

4. MSF with brine mixing (MSF-M)

The MSF-M system is a novel process proposed by El-Dessouky et al. [35]. The main objective of this process is to reduce the energy losses in the cooling seawater stream, found in conventional MSF, or in the large brine blowdown stream, found in MSF-OT. The recovered energy will result in an improvement of the system overall performance.

The process layout, shown in Fig. 4, includes a brine heater; a heat recovery section and a brine recycle mixing tank. A comparison of the process layout (Fig. 4) with that for conventional MSF (Fig. 1) shows the following:

1. removal of the heat rejection section;
2. absence of the cooling water loop used in conventional MSF to control the flashing temperature in the last stage and to remove excess energy added to the system in the brine heater;
3. elimination of the cooling water recycle loop, which is used to adjust the flashing temperature of the seawater of the last flashing stage in the heat rejection section, when the seawater temperature becomes very low during winter operation;
4. the mixing of the brine recycle and the feed seawater takes place in an external mixing tank rather than inside the flashing stages;
5. the salinity of the rejected brine can be less than the limiting value of 70 000 ppm; this depends on the temperature of the feed seawater;
6. the flow rate of the feed seawater is not constant and is regulated subject to the temperature and salinity of the seawater.

Similarly, the differences between MSF-M and MSF-OT include the following:

1. in MSF-M, a portion of the outlet brine from the last stage is circulated back to the system; the recycled stream recovers part of the system energy and, as a result, improves the overall system performance;
2. brine recirculation reduces the flow rate of the feed seawater; consequently lower amounts of chemical additives are used and a smaller sized pretreatment plant is required, which includes screening, filtration and deaeration;
3. the use of the mixing tank for the feed stream and the brine recycle stream gives a better control of the temperature of the brine feed to the condenser tubes of the last flashing stage;
4. the salinity of the recycle brine is higher than that of the feed seawater;
5. deaeration of the feed seawater takes place outside the stage; this reduces the corrosion rate inside the stages;
6. the system is less sensitive to variations in feed seawater temperature because it can be controlled by the brine circulation rate.

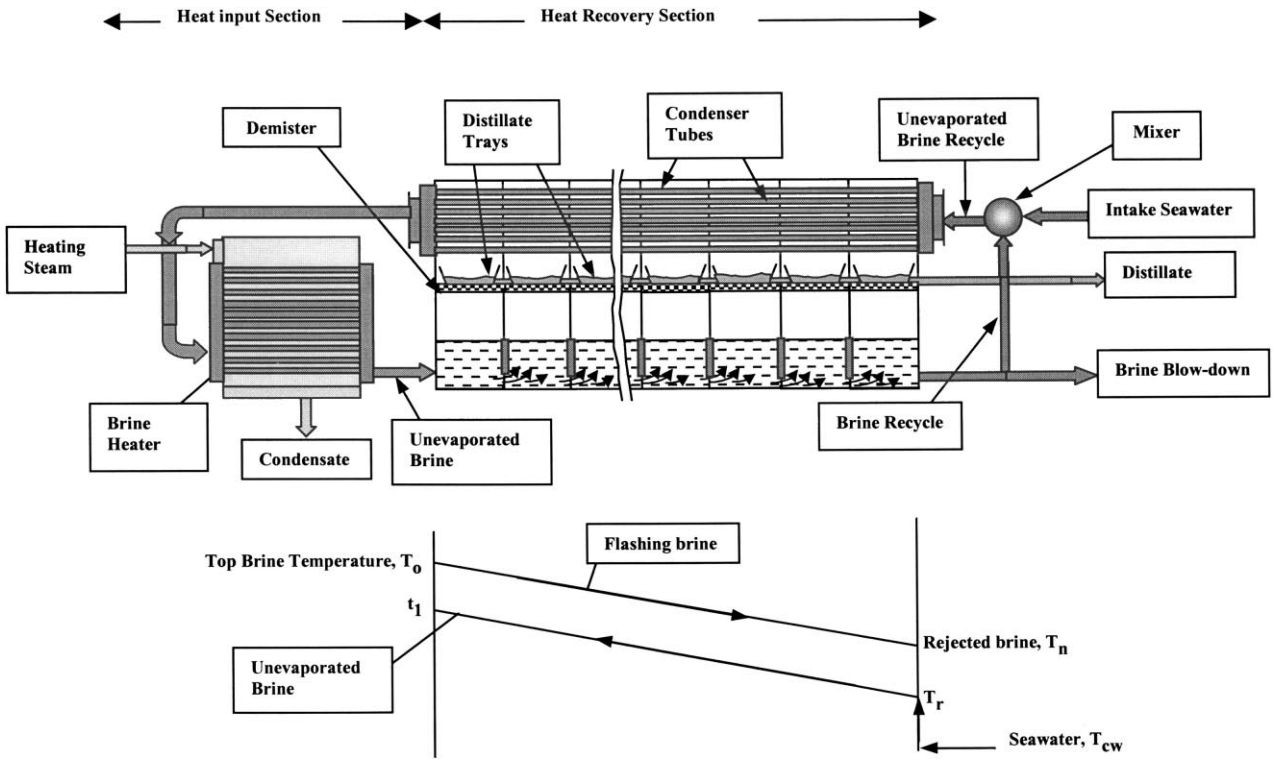

Fig. 4. Schematic of MSF-M desalination plant and temperature profiles.

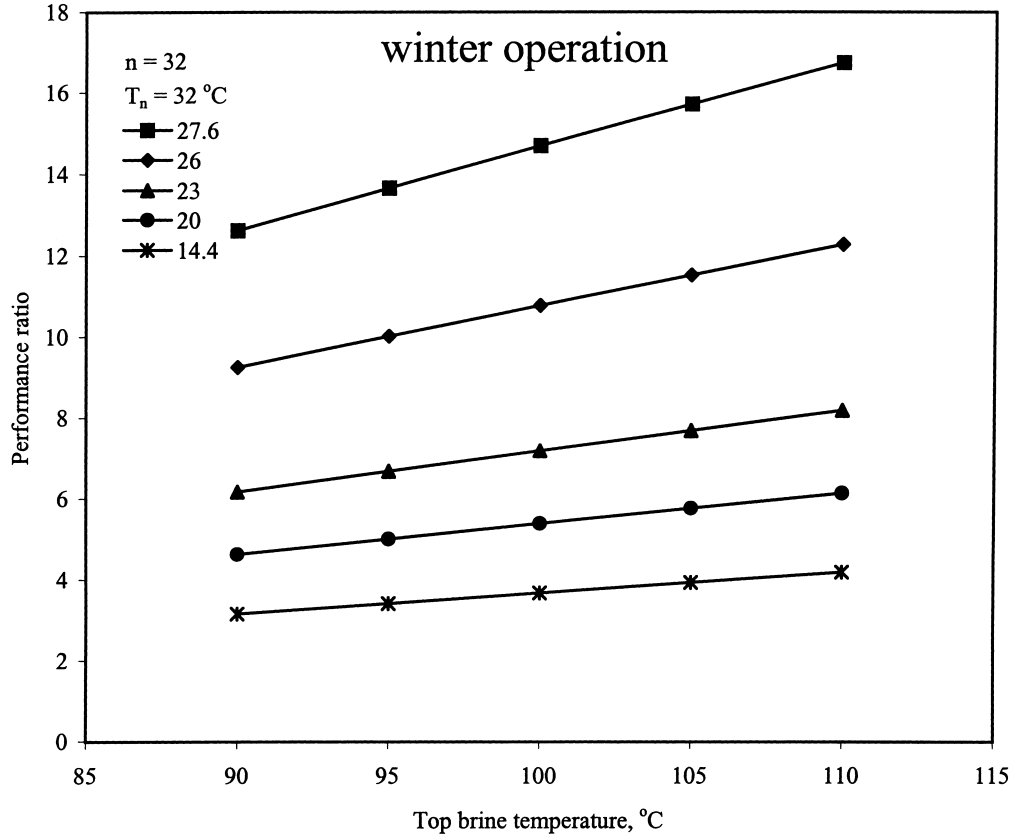

Fig. 5. Effect of the top brine temperature on the performance ratio for different temperatures of the recycled unevaporated brine.

4.1. Performance of MSF-M

The performance of the proposed MSF-M system is analyzed as a function of the top brine temperature, the temperature of the unevaporated brine recycle and the number of stages. The mathematical model given in Appendix C is solved to predict the performance of the MSF-M system. Model predictions and results are shown in Figs. 5–8 for the thermal performance ratio and the total specific heat transfer area. All results correspond to summer operation, except for Fig. 5, which shows the performance ratio for winter operation.

Figs. 5 and 6 display the variations in the thermal performance ratio as a function of the top brine temperature and the temperature of the unevaporated brine recycle. The data in Fig. 5 are for winter operation and in Fig. 6 for summer operation. Variations in the thermal performance ratio of the MSF-M system are similar to those of the conventional MSF system, where the thermal performance ratio increases at higher temperatures of the top brine and the unevaporated brine recycle. A comparison of the data in Figs. 5 and 6 shows comparable performance during winter and summer operation, with an increase in the system thermal performance at higher values of the top brine temperature and the temperature of the unevaporated brine recycle. The results show two main features for the MSF-M system. The first feature occurs for equal temperatures of the unevaporated brine recycle and the feed seawater, i.e. $T_r=T_f$. At this condition, the portion of the brine stream leaving the last flashing stage, which is mixed with the feed stream, is equal to zero. Therefore, the MSF-M system becomes identical to the MSF-OT system. Accordingly, the system thermal performance ratio has lower values, which vary over a range of 3–8, (see Table 2). This is because of the large amount of energy rejected with the brine blowdown. The lower range of the thermal performance is obtained for winter operation, with values between 3–4, and the higher range for summer operation, with values of 5–8. Therefore, adoption of the stand-alone MSF-OT system, as proposed by Wangnick et al. [36], is not feasible because of the very low performance ratios during winter operation and at low top brine temperatures. As a result, a control mechanism must be used to maintain the seawater temperatures at higher values during winter operation and at low top brine temperature. This control mechanism is found in the heat rejection section in conventional MSF and in the brine mixing tank in the MSF-M system. The second feature occurs as the temperature of the unevaporated brine recycle, T_r, is increased to higher values, where a two- to threefold increase occurs in the thermal performance ratio. This large increase in the thermal performance ratio is caused by the increase in the flow rate and temperature of the unevaporated brine recycle. Therefore, a larger amount of energy is recovered by the system and,

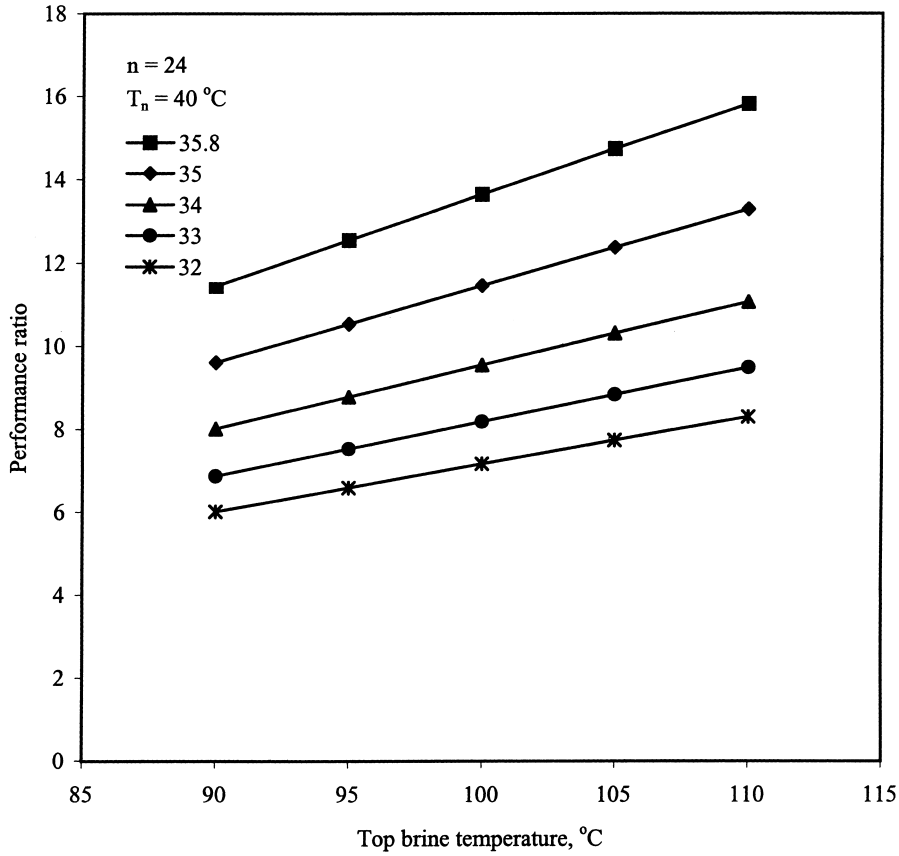

Fig. 6. Effect of the top brine temperature on the performance ratio for different temperatures of the recycled unevaporated brine.

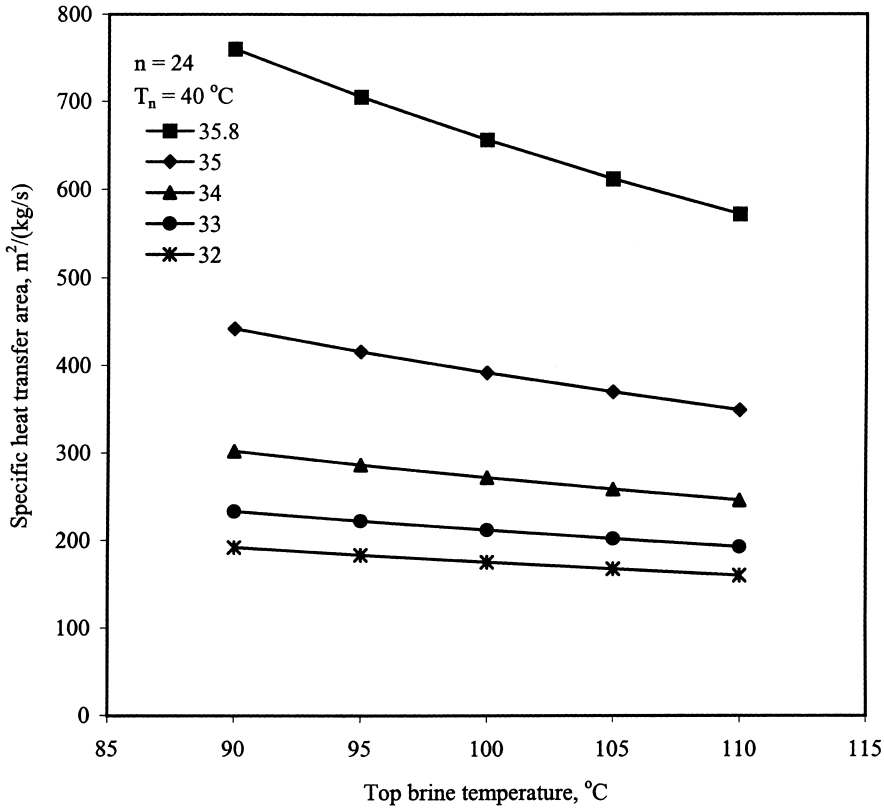

Fig. 7. Effect of the top brine temperature on the specific heat transfer area for different temperatures of the recycled unevaporated brine.

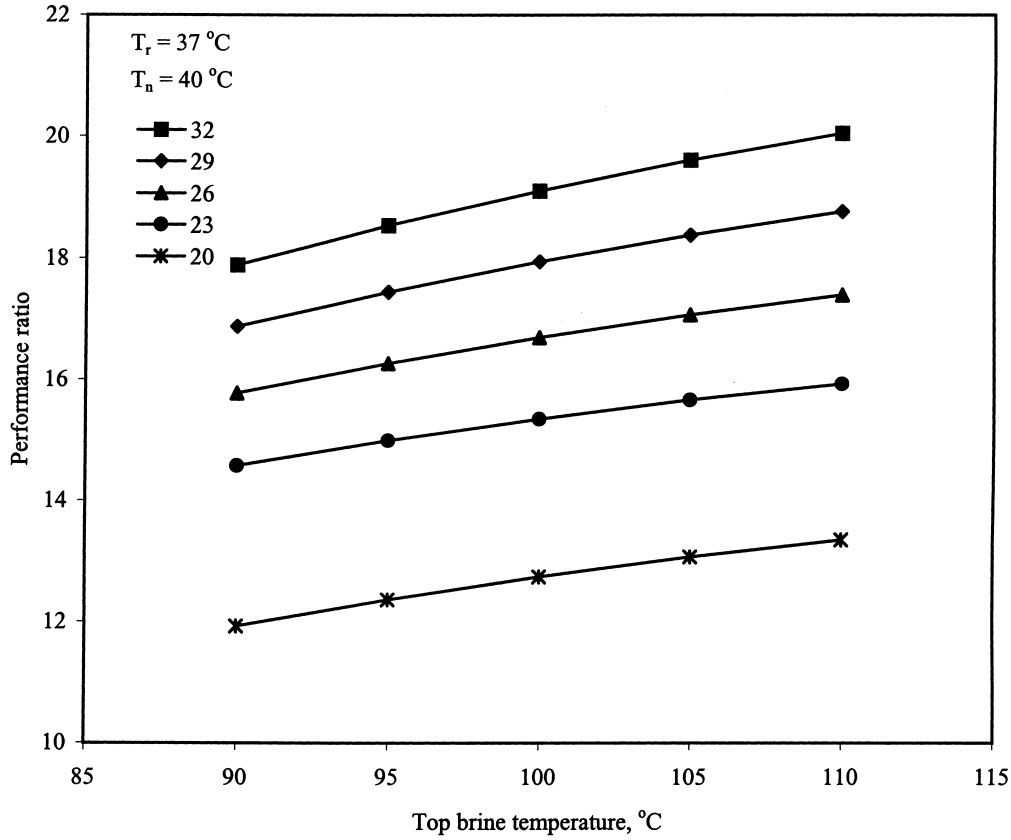

Fig. 8. Effect of the top brine temperature and the number of stages on the performance ratio.

consequently, the process consumes a smaller amount of steam.

The results for the specific heat transfer area are shown in Fig. 7. As illustrated, the heat transfer area decreases with an increase in the top brine temperature and a decrease in the temperature of the unevaporated brine recycle. The increase in the top brine temperature gives a larger flashing range, which results in an increase in the stage temperature drop. At a higher stage temperature drop, the driving force for heat transfer is higher. This results in a reduction in the heat transfer area. In addition, at higher brine temperatures the overall heat transfer coefficient is larger; this reduces the required heat transfer area. At lower temperatures of the unevaporated brine recycle, the temperature difference between the brine flowing inside the condenser/preheater tubes and the condensing vapor is high; this increases the temperature driving force for heat transfer and consequently reduces the heat transfer area. At low temperatures of the unevaporated brine recycle, the values of the total specific heat transfer area are consistent with the conventional MSF system. At higher temperatures of the unevaporated brine recycle, the total specific heat transfer area increases due to a reduction in the heating temperature driving force.

The effects of the number of flashing stages on the performance of the MSF-M system are shown in Fig. 8. The results were obtained at a temperature of 37°C for the unevaporated brine recycle. The results in Fig. 8 show that the performance ratio of the MSF-M system is higher by a factor of two than that of the conventional MSF system with brine recirculation. Further, operation at larger number of stages increases the MSF-M performance ratio by a factor of three. As for the total specific heat transfer area, its value varies at similar rates as the number of stages increases.

4.2. Modification of existing MSF plants to MSF-M

Conversion of the MSF system with brine recirculation to the MSF-M configuration is simple and primarily involves elimination of the brine circulation and cooling seawater streams. The conversion includes the following:

1. removal of the cooling seawater loop as well as the temperature control loop on the feed seawater temperature;
2. modification of the brine circulation loop to recycle the brine to the storage tank instead of to the last stage;
3. addition of the accumulation tank for the recycled brine stream;
4. connection of the preheater tubes of the first stage in the heat rejection section and the last stage in the heat recovery section;
5. replacement of the intake seawater pump with a smaller capacity pump; this is necessary because the cooling seawater stream in the MSF-M system is eliminated.

Table 1
Design parameters for a typical MSF system with brine recirculation

Variables	Brine heater	Heat recovery section	Heat rejection section
No. of stages	1	21	3
No. of tubes/stages	1378	1451	1588
Heat transfer area (m^2)	3544	77206	9444
Heat transfer coefficient			
U^* (high/low) (kW $m^{-2}{}^\circ C^{-1}$)	4.476/4.537	4.788/4.6293	3.894/3.742
U^{**} (high/low) (kW $m^{-2}{}^\circ C^{-1}$)	2.055/2.068	2.7934/2.7385	2.3119/2.25748
Fouling factor	2.63×10^{-4}	1.4915×10^{-4}	1.757×10^{-4}

Type of antiscalant: Sokalan PM 10i.
Dosing rate 4 g per ton of make-up seawater.
* Clean.
** Unclean.

5. Comparison of conventional MSF, MSF-OT and MSF-M

Comparison of the three MSF configurations is performed for the design data given in Table 1. For the conventional MSF system, the reduction in the temperature of the intake seawater has no effect on the system thermal performance ratio. This is because the temperature of the intake seawater is adjusted in the heat rejection section, where it increases from 14.4°C to 35.18°C during winter operation and from 32.22°C to 40.5°C during summer operation. As shown in Table 2, the adjustment in the steam temperature, during winter and summer operation, keeps the flashing range constant. Therefore, the system performance ratio varies over a narrow range of 8–8.65 for low and high capacity operation and during the summer and winter seasons.

The opposite behavior is found for MSF-OT, where the thermal performance ratio of the system varies over a wider range, with lower values of 3–4 during winter operation and 5.82–7.3 during summer operation. This is caused by the absence of a control mechanism on the temperature of the intake seawater i.e. the heat rejection section in the conventional MSF system and the mixing tank in the novel MSF-M system. The low temperature of the intake seawater, 14.4°C, causes the low performance ratio for the MSF-OT system during the winter.

As shown in Table 2, the thermal performance ratio for the MSF-M system varies over a wider and higher range than for the other two systems. The system performance ratio for winter operation is 12, which is higher than the conventional MSF system by 50%. This value increases to 16 in summer operation, which is higher by 100% than the MSF system. The performance ratio for the MSF-M system is limited by the maximum salinity value imposed on the brine blowdown stream as well as the terminal temperature difference. For example, reduction of the intake seawater salinity to a value of 34 000 ppm, typical of large water bodies, allows for an increase in the temperature of the unevaporated brine recycle to higher values during winter operation and an increase in the system thermal performance ratio to values close to 16.

Brine circulation in the proposed MSF-M and conventional MSF systems gives similar consumption rates of the antiscalant material, with values ranging between 0.00314 and 0.00455 kg s^{-1}. The opposite behavior is found for the MSF-OT system, where absence of a brine circulation stream necessitates the treatment of a much larger feed seawater stream. As a result, the consumption rate of the antiscalant for the MSF-OT system is higher by a factor of 3–4, with values ranging from 0.011 to 0.014 kg s^{-1}.

6. Conclusions

The present performance and future outlook for the MSF process have been analyzed through a detailed discussion of the process fundamentals and performance of a novel MSF configuration. The process fundamentals have involved an analysis of the interactions and functions of various MSF elements, including the flashing stage, the once-through arrangement, the cooling seawater stream, the brine recycle and the heat rejection section. An analysis has been presented for the single effect flashing stage, the once-through system, the novel brine mixing configuration and the conventional MSF system.

The novel brine-mixing MSF process, MSF-M, presented in this study contains the main elements of the conventional MSF system. This allows for simple modification of operational MSF units to the newly proposed MSF-M system. The MSF-M system gives higher thermal performance ratios with values ranging between 12 and 20. This increase is caused, in part, by a reduction in the amount of energy rejected in the cooling seawater stream. This reduces the amount of heating steam needed by the system, which, in turn, increases the system thermal performance ratio.

The characteristics of the MSF-M system can be summarized as follows:

1. the thermal performance ratio of the MSF-M system is twofold higher than that of conventional MSF as the temperature of the unevaporated brine recycle ap-

Table 2
Comparison of different configurations

Parameter	Low temperature			High temperature		
	MSF	Once-through	MSF-M	MSF	Once-through	MSF-M
Summer operation						
Capacity (kg s^{-1})	313.25	313.25	313.25	375.92	375.92	375.92
Seawater temperature (°C)	32.22	32.22	32.22	32.22	32.22	32.22
Temperature of recirculated brine (°C)	40.5	–	36.22	40.5	–	37.84
Last stage brine temperature (°C)	40.5	40.5	40.5	41.21	41.21	41.21
Product water temperature (°C)	38.6	40	40	39.3	40.71	40.71
Brine heater inlet temperature (°C)	84.89	82.28	87.97	103.02	101.01	106.63
Top brine temperature (°C)	90.56	90.56	90.56	110	110	110
Steam temperature (°C)	100	100	100	119.85	119.85	119.85
Cooling water flow rate (kg s^{-1})	1862.19	0	0	1523.89	0	0
Brine recirculation rate (kg s^{-1})	3968.3	0	3510.77	3476.4	0	3032.68
Blowdown flow rate (kg s^{-1})	499.36	3179.52	784.93	551.94	2656.76	760.911
Make-up water flow rate (kg s^{-1})	812.6	3510.77	1098.18	927.78	3032.68	1136.83
Heating steam flow rate (kg s^{-1})	39.16	53.86	16.85	43.46	51.75	19.4
Antiscalant consumption rate (kg s^{-1})	0.00325	0.01404	0.00439	0.00371	0.01213	0.00455
Brine circulation ratio	12.67	0	11.2	9.25	0	8.07
Flashing range (°C)	50.06	50.06	50.6	68.79	68.79	68.8
Total temperature range (°C)	58.34	58.34	58.34	77.78	77.78	77.78
Peformance ratio	8	5.82	18.6	8.65	7.3	19.4
Salt concentration in circulated brine (ppm)	61 500	–	53 518.4	61 500	–	54971.4
Salt concentration of feed water (ppm)	42 000	42 000	42 000	42 000	42 000	42 000
Salf concentration of rejected brine (ppm)	70 000	46 115	58 761	70 000	47 943	62 750
Winter operation						
Capacity (kg s^{-1})	313.25	313.25	313.25	375.92	375.92	375.92
Seawater temperature (°C)	14.4	14.4	14.4	14.4	14.4	14.4
Temperature of recirculated brine (°C)	35.18	–	27.62	35.18	–	26.01
Last stage brine temperature (°C)	35.18	32	32	35.18	32	32
Product water temperature (°C)	33.18	31.5	31.5	33.18	31.5	31.5
Brine heater inlet temperature (°C)	82.13	70.48	83.7	100.59	90.34	101.95
Top brine temperature (°C)	88.08	88.08	88.08	107.94	107.94	107.94
Steam temperature (°C)	97.59	97.59	97.59	117.78	117.78	117.78
Cooling water flow rate (kg s^{-1})	1003.8	0	0	910.83	0	0
Brine recirculation rate (kg s^{-1})	3795.3	0	3152.2	3314.2	0	2764.09
Blowdown flow rate (kg s^{-1})	494.3	2838.95	471.22	544.2	2388.17	564.813
Make-up water flow rate (kg s^{-1})	807.6	3152.2	784.5	920	2764.09	940.733
Heating steam flow rate (kg s^{-1})	39.16	102.5	25.5	43.46	92.09	31.35
Antiscalant consumption rate (kg s^{-1})	0.00323	0.01261	0.00314	0.00368	0.01106	0.00376
Brine circulation ratio	12.12	–	10.06	8.82	–	7.35
Flashing range (°C)	52.9	56.08	56.08	72.72	75.94	75.94
Total temperature range (°C)	73.68	73.64	73.64	93.54	93.54	93.54
Peformance ratio	8	3.06	12.28	8.65	4.08	11.99
Salt concentrate in circulated brine (ppm)	61 500	–	62 971.9	61 500	–	60 439.9
Salt concentrate of feed water (ppm)	42 000	42 000	42 000	42 000	42 000	42 000
Salf concentrate of rejected brine (ppm)	70 000	46 634	69 920	70 000	48 611	69 954

proaches the temperature of the brine blowdown and for a number of stages greater than 23;

2. the salinity of the unevaporated brine recycle and brine blowdown has a lower value than that of conventional MSF over a wide range of top brine temperatures, number of stages and temperature of the unevaporated brine recycle;
3. an increase in the MSF-M performance ratio during summer operation gives the system a distinct advantage over the MSF system, because of the increase in per capita consumption of water and electricity; this reduces the capital as well as operating costs and, in turn, reduces the unit production cost;
4. operation of the MSF-M system with no brine recycle reduces the system to the MSF-OT configuration, which has a much lower thermal performance ratio, especially during winter operation;
5. brine circulation in the MSF-M system gives a similar consumption rate of antiscalant as for the MSF system; as the MSF-OT system has no brine recycle stream, its antiscalant consumption rate is 3–4 times higher than that of the other two systems.

The important factor addressed in this study is the need to increase the thermal performance ratio beyond the value of eight. This is a must in order to face the challenges of other competitive thermal desalination processes. The proposed system, MSF-M, shows that innovative design can lead to the desired system performance.

Appendix A

Nomenclature

A	heat transfer surface area (m^{-2})
B	flashing brine (kg s^{-1})
BPE	boiling point elevation (°C)
C_d	gate discharge coefficient
C_p	specific heat at constant pressure (kJ kg^{-1}°C)
D	distillate product (kg s^{-1})
GH	gate height (m)
h	heat transfer coefficient (kW m^{2}°C)
j	number of heat rejection stages
k	thermal conductivity (kW m^{-1}°C)
L	stage length (m)
LMTD	logarithmic mean temperature difference (°C)
M	mass flow rate (kg s^{-1})
n	total number of stage
NEA	non-equilibrium allowance (°C)
P	pressure (kPa)
PR	thermal performance ratio, (kg of distillate/kg of motive steam)
r	tube radius (m)
R_f	fouling factor heat resistance (m^{2}°C KW^{-1})
sA	specific heat transfer surface area (m^2 kg^{-1} s^{-1})
sM_{cw}	specific cooling water flow rate (dimensionless)
sM_f	specific feed water flow rate (dimensionless)
t	brine temperature flowing inside the condenser tubes (°C)
T	temperature (°C)
TTD	terminal temperature difference (°C)
Δt	temperature drop of unevaporated brine (°C)
ΔT	temperature drop of flashing brine (°C)
U	overall heat transfer coefficient (KW m^{-2}°C)
V	velocity (m s^{-1})
W	stage width (m)
X	salt concentration (ppm)

Greek letters

λ	latent heat of vaporization (kJ kg^{-1})
ρ	density (kg m^{-3})

Subscripts

b	reject brine
c	condensers in heat recovery section
cw	intake seawater
d	product freshwater
f	feed seawater
h	brine heater
i	tube inside
j	condensers in heat rejection section
loss	thermodynamic losses
n	stage n
o	tube outside or outlet stream
p	demister
r	recycle brine
s	heating steam
st	stage temperature drop
v	condensing vapor
w	tube wall

Appendix B

Analytical models of MSF configurations

The following mathematical model contains the basic elements used for the various MSF configurations. The model contains total mass and salt balances, rate equations for the heat transfer units and energy balances for the brine heater and the condenser. The total mass and salt balances are

$$M_f = M_b + M_d, \tag{B.1}$$

$$X_f M_f = X_b M_b, \tag{B.2}$$

where M is the mass flow rate, X the salt concentration, and the subscripts b, d, and f denotes the brine, distillate, and feed streams, respectively.

The brine heater and condenser energy balances are given, respectively, by

$$M_s \lambda_s = M_f C_p (T_o - t_1), \tag{B.3}$$

$$M_d \lambda_v = M_f C_p (T_o - T_n), \tag{B.4}$$

where C_p is the specific heat at constant pressure, T the temperature of the flashing brine, t the temperature of the seawater flowing in the condenser tubes, λ the latent heat of evaporation, the subscripts o and 1 define the brine stream entering and leaving the first stage, and the subscripts s and v denote the heating steam and the flashing vapor. The heat transfer rate equation for the brine heater is

$$M_s \lambda_s = U_h A_h (\mathrm{LMTD})_h, \tag{B.5}$$

where

$$(\mathrm{LMTD})_h = (T_o - t_1)/\ln[(T_s - t_1)/(T_s - T_o)]. \tag{B.6}$$

The heat transfer rate equation for the condenser is

$$M_f C_p (t_1 - t_2) = U_c A_c (\mathrm{LMTD})_c, \tag{B.7}$$

where

$$(\mathrm{LMTD})_c = (t_1 - t_2)/\ln[(T_{v_1} - t_2)/(T_{v_1} - t_1)]. \tag{B.8}$$

In the above system of equations, A is the heat transfer area, LMTD is the logarithmic mean temperature difference, U is the overall heat transfer coefficient and the subscripts c and h denote the condenser and the brine heater, respectively. The unit thermal performance ratio, defined as the mass ratio of freshwater produced per unit mass of heating steam, is obtained by dividing Eqs. (B.4) and (B.3), where

$$\mathrm{PR} = \frac{M_\mathrm{d}}{M_\mathrm{s}} = \frac{M_\mathrm{f} C_\mathrm{p}(T_\mathrm{o} - T_n)\lambda_\mathrm{s}}{M_\mathrm{f} C_\mathrm{p}(T_\mathrm{o} - t_1)\lambda_\mathrm{v}} = \frac{(T_\mathrm{o} - T_n)\lambda_\mathrm{s}}{(T_\mathrm{o} - t_1)\lambda_\mathrm{v}}. \tag{B.9}$$

The temperature difference $(T_\mathrm{o}-T_n)$ gives the stage temperature drop, $n\Delta T_\mathrm{st}$, which is known as the stage flashing range. On the other hand, the term $(T_\mathrm{o}-t_1)$, as is shown in Fig. 3, is equal to the sum of the stage temperature drop, ΔT_st, the condenser terminal temperature difference, $\mathrm{TTD_c}$, and the thermodynamic loss, ΔT_loss, or,

$$(T_\mathrm{o} - T_1) = \Delta T_\mathrm{st}, \text{ and}$$

$$(T_\mathrm{o} - t_1) = \Delta T_\mathrm{st} + \Delta T_\mathrm{loss} + \mathrm{TTD_c}.$$

The thermodynamic loss, ΔT_loss, is given by the temperature difference between the brine leaving the stage, T_1, and the condensation temperature of the vapor, T_{v_1}. This loss is caused by non-equilibrium allowance, boiling point elevation and temperature depression due to the pressure drop in the demister and the condenser. The above two relations are substituted in Eqs. (B.3)–(B.9), resulting in

$$M_\mathrm{s}\lambda_\mathrm{s} = M_\mathrm{f} C_\mathrm{p}(\Delta T_\mathrm{st} + \Delta T_\mathrm{loss} + \mathrm{TTD_c}), \tag{B.10}$$

$$M_\mathrm{d}\lambda_\mathrm{v} = M_\mathrm{f} C_\mathrm{p}(n\Delta T_\mathrm{st}), \tag{B.11}$$

$$(\mathrm{LMTD})_\mathrm{h} = (\Delta T_\mathrm{st} + \Delta T_\mathrm{loss} + \mathrm{TTD_c})/\ln [(\Delta T_\mathrm{st} + \Delta T_\mathrm{loss} + \mathrm{TTD_c} + \mathrm{TTD_h})/(\mathrm{TTD_h})], \tag{B.12}$$

$$M_\mathrm{f} C_\mathrm{p} \Delta T_\mathrm{st} = U_\mathrm{c} A_\mathrm{c} (\mathrm{LMTD})_\mathrm{c}, \tag{B.13}$$

$$(\mathrm{LMTD})_\mathrm{c} = (\Delta T_\mathrm{st})/\ln[(\Delta T_\mathrm{st} + \mathrm{TTD_c})/(\mathrm{TTD_c})], \tag{B.14}$$

$$\mathrm{PR} = \frac{n\Delta T_\mathrm{st}\lambda_\mathrm{s}}{(\Delta T_\mathrm{st} + \Delta T_\mathrm{loss} + \mathrm{TTD_c})\lambda_\mathrm{v}}, \tag{B.15}$$

Eqs. (B.1), (B.2), (B.10)–(B.15) are used to analyze various flashing configurations.

The mathematical model for the MSF-M system is similar to that given above; however, two additional balance equations are made for the recycle brine mixer. The equations include a mixer energy balance and salt balance, where

$$(M_\mathrm{r} - M_\mathrm{f}) C_\mathrm{p}(T_n - T_\mathrm{cw}) = M_\mathrm{r} C_\mathrm{p}(T_\mathrm{f} - T_\mathrm{cw}), \tag{B.16}$$

$$M_\mathrm{r} X_\mathrm{r} = X_\mathrm{f} M_\mathrm{f} + X_n(M_\mathrm{r} - M_\mathrm{f}). \tag{B.17}$$

The MSF model contains additional equations for the recycle salt balance, the cooling water energy balance and the temperature drop in the condensers in the rejection section. These equations are as follows:

$$X_\mathrm{r} = [(X_\mathrm{f} - X_\mathrm{b})M_\mathrm{f} + M_\mathrm{r} X_\mathrm{b}]/M_r, \tag{B.19}$$

$$M_\mathrm{cw} = [M_\mathrm{s}\lambda_\mathrm{s} - M_\mathrm{f} C_\mathrm{p}(T_n - T_\mathrm{cw})]/(C_\mathrm{p}(T_n - T_\mathrm{cw})], \tag{B.20}$$

$$\Delta t_j = (T_n - T_\mathrm{cw})/j. \tag{B.21}$$

Appendix C

Detailed mathematical model of MSF-M

A detailed mathematical model is developed to simulate and analyze the proposed MSF-M system. It was necessary to adopt a detailed model rather than a simplified analytical procedure to avoid inaccurate predictions, which may lead to results and behavior inconsistent with known practice.

The main feature of the developed mathematical model is that the heat transfer area is equal in all flashing stages. This is the basic practice in the desalination industry, because it reduces design and construction costs and the stocking of spare parts. Other model features include the following:

1. the inclusion of distillate flashing as it flows through the stages and its heating effect on the seawater stream flowing inside the condenser/preheater tubes;
2. the consideration of the effects of boiling point elevation, temperature depression corresponding to the pressure drop in the demister and during condensation and the non-equilibrium allowance on the temperature of the flashing vapor;
3. the consideration of the presence of non-condensable gases and their effects on the value of the heat transfer coefficient;
4. the thermophysical properties are a function of the stream composition and temperature; these properties include the specific heat, density, viscosity, thermal conductivity, vapor saturation temperature and pressure, and latent heat;
5. the dependence of the overall heat transfer coefficients on the fluid properties, presence of non-condensable gases, fluid phase and tube geometry and configuration;
6. the boiling point elevation and the non-equilibrium allowance are calculated as a function of the stream properties; the non-equilibrium allowance also depends on the stage geometry.

On the other hand, a number of simplifying assumptions are adopted in model development. As discussed below, these assumptions have a negligible effect on the accuracy of model predictions; however, they facilitate mathematical development, the solution procedure and the computational effort. These assumptions are:

1. the distillate product is salt free; this assumption is valid since the boiling temperature of water is much lower than that of the salts;

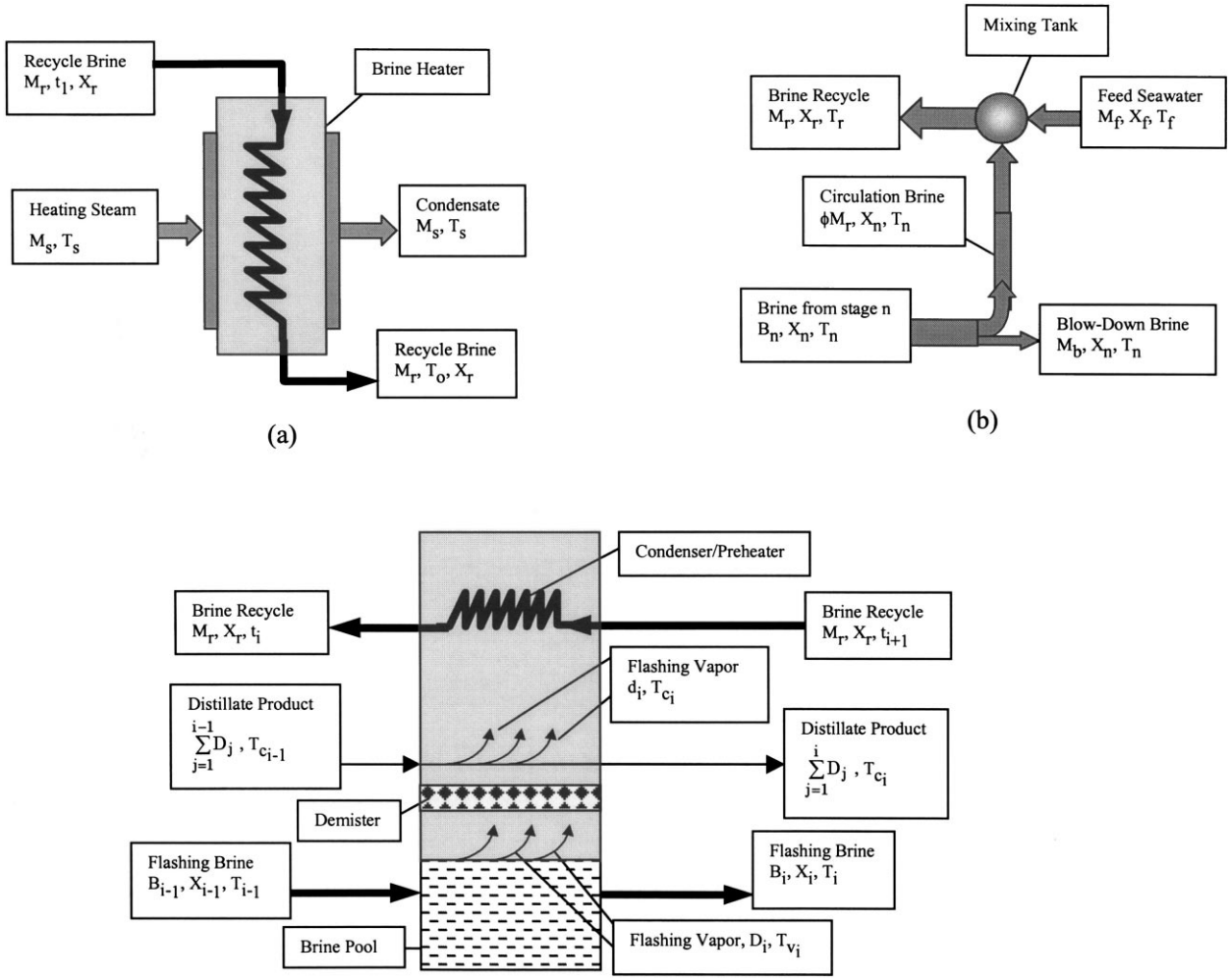

Fig. 9. Schematics of model variables in MSF-M, (a) brine heater, (b) mixer of circulating brine, and (c) flashing stage.

2. the subcooling of the condensate or the superheating of the heating steam has a negligible effect on the system energy balance; this is because of the large difference between the vapor latent heat and the sensible heat value caused by liquid subcooling or vapor superheating of a few degrees.
3. the power requirements for pumps and auxiliaries are not considered in the system analysis; this power has no effect on the accuracy of prediction of the system thermal performance ratio, which depends only on the consumption rate of the heating steam;
4. the heat losses to the surroundings are negligible, because the flashing stages and the brine heater are usually well insulated and operate at relatively low temperatures.

Fig. 9 shows the process variables for the brine heater, the mixing tank and the flashing stage.

The stage model equations include balances for energy, total mass, and salt. The stage total mass balance is given by

$$B_{i-1} + \sum_{j=1}^{i-1} D_j = B_i + \sum_{j=1}^{i} D_j.$$

The above relation simplifies to

$$D_i = B_{i-1} - B_i, \tag{C.1}$$

where B and D are the flow rates of the flashing brine and distillate product and the subscripts i and $i-1$ are the stage numbers. It should be noted that the term B_{i-1} in Eq. (C.1) for the first flashing stage is equal to M_f. The stage salt balance is given by

$$X_i B_i = X_{i-1} B_{i-1}. \tag{C.2}$$

The stage energy equations include balances for the flashing brine, the preheater/condenser unit and the total balance. The energy balance for the flashing brine is

$$D_i \lambda_{v_i} = B_{i-1} C_p (T_{i-1} - T_i). \tag{C.3}$$

In the above equation, the term, λ_{v_i}, is the latent heat of the flashing vapor and is calculated at the vapor temperature, T_{v_i}. This temperature is lower than the stage temperature T_i

by the thermodynamic losses, where

$$T_i = T_{v_i} + \mathrm{BPE}_i + \mathrm{NEA}_i. \tag{C.4}$$

The boiling point elevation, BPE, is dependent on the brine salinity and its boiling temperature. On the other hand, the non-equilibrium allowance, NEA, gives a measure of the flashing process thermal efficiency. The non-equilibrium allowance depends on the stage flashing range, T_i–T_{i+1}, the stage saturation temperature, T_{vi}, the flow rate of the brine recycle, the stage width, and the height of the brine pool.

The energy balance on the condenser/preheater tubes is given by

$$D_i\lambda_{v_{c_i}} + C_p\left(T_{v_{c_{i-1}}} - T_{v_{c_i}}\right)\sum_{j=1}^{i-1} D_j = M_r C_p(t_i - t_{i+1}), \tag{C.5}$$

where $\lambda_{v_{c_i}}$ is the latent heat of condensing vapor at the condensation temperature, $T_{v_{c_i}}$. The second term on the left-hand side of Eq. (C.5) accounts for reduction in the distillate temperature as it flows across the stages. It should be noted that, in the first stage, the term $\sum_{j=1}^{i-1} D_j$ is equal to zero. The saturation temperature, $T_{v_{c_i}}$, is less than the stage saturation temperature, T_{v_i}, by the temperature depression caused by pressure losses in the demister pad and around the condenser tubes. This is pressure drop is given by

$$\Delta P = \Delta P_p + \Delta P_c. \tag{C.6}$$

In MSF flashing units, the pressure loss around the condenser tubes is equal to the sum of the friction losses and the pressure gain due to gas deceleration. In typical MSF units, the two terms of pressure loss and gain are nearly of the same magnitude and can cancel each other. Therefore, the pressure drop experienced by the flashing vapor is out primarily due to the demister pads, [33]. The expression for the pressure drop in the demister pad was previously developed by El-Dessouky et al. [37].

The stage overall energy balance conserves the energies of the input and output streams of the flashing brine, product distillate and brine recycle flowing in the condenser tubes. This balance is

$$B_i C_p T_i + C_p T_{vi}\sum_{j=1}^{i} D_j + M_r C_p t_i = B_{i-1} C_p T_{i-1} + C_p T_{vi-1}\sum_{j=1}^{i-1} D_j + M_r C_p t_{i+1}. \tag{C.7}$$

The heat transfer areas are calculated for both the preheater/condenser tubes in each stage and in the brine heater. The rate equations for the brine heater have been given previously by Eqs. (B.5) and (B.6). Similarly, the equations for the preheater/condenser heat transfer area are given by Eqs. (B.7) and (B.8).

The following known relation expresses the overall heat transfer coefficient, U, in terms of the various resistances encountered for heat transfer from the vapor condensing outside the tubes to the brine stream flowing inside the tubes,

$$\frac{1}{U_o} = \frac{1}{h_i}\frac{r_o}{r_i} + R_{f_i}\frac{r_o}{r_i} + \frac{r_o \ln(r_o/r_i)}{k_w} + R_{f_o} + \frac{1}{h_o}. \tag{C.8}$$

Details of all the terms in Eq. (C.8) have been given previously by El-Dessouky and Bingulac [33]. The overall heat transfer coefficients for the brine heater and the preheater/condenser tubes are similar, where the seawater flows inside the tubes and the vapor condenses on the outside surface. The following correlation was developed by El-Dessouky, et al. [12]:

$$U = 1.7194 + 3.2063\times10^{-3}T + 1.5971\times10^{-5}T^2 - 1.9918\times10^{-7}T^3. \tag{C.9}$$

In the above equation, U is the overall heat transfer coefficient in kW $m^{-2}{}^{\circ}C^{-1}$, and T is the vapor condensation temperature in °C. The above equation was developed over a temperature range of 40–120°C.

The stage design parameters include the stage length, L, the stage width, W, the gate height, GH, and the height of the brine pool, H. Common design practice adopts the width of the first stage and the length of the last stage for all other stages. This is because the stage width depends on the flow rate of the flashing brine, which has a maximum value in the first stage. Also, the stage length depends on the vapor specific volume, which has a maximum value in the last stage. The stage width, W, is obtained from the following relation

$$W = M_r/V_b, \tag{C.10}$$

where W is the stage width and V_b is the brine flow rate per unit width with a maximum value of 0.3611 $m^3\,s^{-1}\,m^{-1}$, [36]. The equation for the stage length, L, is given by

$$L = D_n/(\rho_{vn}V_{vn}W), \tag{C.11}$$

where ρ_v is the vapor density and V_v is the velocity of flashed off vapor. The height of the brine pool, H, is higher than the sluice gate height, GH, by 0.1–0.2 m. The gate height is obtained from

$$\mathrm{GH}_i = \left(M_r - \sum_{j=1}^{i-1} D_j\right)(2\rho_{bi}\Delta P_i)^{(-0.5)}/(C_d W), \tag{C.12}$$

where ΔP is the pressure of stages i and i+1 and C_d is the gate discharge coefficient. It should be noted that the gate varies from one stage to another. On the other hand, the height of the brine pool varies only slightly between adjacent stages.

References

[1] G.F. Leitner, Is there a water crisis? Int. Desalination & Water Reuse Quart. 7 (1998) 10–21.

[2] T.G. Temperley, The coming age of desalination, Proceedings of the IDA World Congress on Desalination and Water Sciences, vol. I, Abu-Dhabi, UAE, November 1995, pp. 219–228.
[3] K. Wangnick, IDA Worldwide Desalting Plants Inventory, report no. 14, 1996.
[4] D.M.K. Al-Gobaisi, A quarter-century of seawater desalination by large multistage flash plants in Abu Dhabi, Desalination 99 (1994) 483–508.
[5] J. Bednarski, M. Minamide, O.J. Morin, Test program to evaluate and enhance seawater distillation process for the metropolitan water district of southern California, Proceedings of the IDA World Congress on Desalination and Water Sciences, vol. I, Madrid, Spain, October 1997, pp. 227–241.
[6] T.M. Leahy, Pipeline versus desalting, Virginia Beach, Virginia, Int. Desalination & Water Resuse 7 (1998) 2832.
[7] N.M. Wade, Technical and economic evaluation of distillation and reverse osmosis desalination processes, Desalination 93 (1993) 343–363.
[8] O.J. Morin, Design and operating comparison of MSF and MED systems, Desalination 93 (1993) 69–109.
[9] J.M. Veza, Mechanical vapour compression desalination plants – a case study, Desalination 101 (1995) 1–10.
[10] C. Temstet, G. Canton, J. Laborie, A. Durante, A large high-performance MED plant in Sicily, Desalination 105 (1996) 109–114.
[11] H.T. El-Dessouky, H.M. Ettouney, Hybrid multiple effect evaporation/heat pump water desalination systems, IDA Seminar, Cairo, Egypt, September 1997.
[12] H.T. El-Dessouky, I.M. Alatiqi, S. Bingulac, H. Ettouney, Steady state analysis of multiple-effect evaporation desalination process, Chem. Eng. Tech. 21 (1998) 15–29.
[13] J. De Gunzbourg, D. Larger, Cogeneration applied to very high efficiency thermal seawater desalination plants, a concept, Int. Desalination & Water Reuse Quart. 7 (1998) 38–41.
[14] Z. Zimerman, Development of large capacity high efficiency mechanical vapor compression (MVC) units, Desalination 96 (1994) 51–58.
[15] H. El-Dessouky, Modeling and simulation of thermal vapor compression desalination plant, Proceedings of the Symposium on Desalination of Seawater with Nuclear Energy, Taejon, Republic of Korea, May 1997.
[16] F. Al-Juwayhel, H. El-Dessouky, H. Ettouney, Analysis of single-effect evaporator desalination systems combined with vapor compression heat pumps, Desalination 114 (1997) 253–275.
[17] H. El-Dessouky, H. Ettouney, Single effect thermal vapor compression desalination process: thermal analysis, J. Heat Eng. (1999), in print.
[18] H.M. Ettouney, H.T. El-Dessouky, Y. Al-Roumi, Analysis of mechanical vapor compression desalination process, Int. J. Energy Res. (1999), in print.
[19] H.T. El-Dessouky, T.A. Khalifa, Scale formation and its effect on the performance of once through MSF plant, Desalination 65 (1985) 199–217.
[20] E.A. Al-Sum, S. Aziz, A. Al-Radif, M. Samir, Heikal, vapour-side corrosion of copper base condenser tubes of the MSF desalination plants of Abu Dhabi, Desalination 97 (1994) 109–119.
[21] M.A. Marwan, N.H. Aly, M.S. Saadawy, Simple code for the estimation of scaling potential, Desalination 101 (1995) 279–286.
[22] A.U. Malik, T.L. Prakash, I. Andijani, Failure evaluation in desalination plants some case studies, Desalination 105 (1996) 283–295.
[23] M.H.A. El-Saie, M.S.I. Kafrawi, M.I. Kamel, Study of the operating conditions for three large MSF desalination units each of capacity 7.2/8. MGD (27360/32832 Ton/Day) in Abu Dhabi, UAE, Desalination 73 (1989) 207–230.
[24] A.U. Malik, P.C. Kutty, I.N. Mayan, S.A. Andijani, Al-Fozan, materials performance and failure evaluation in SWCC MSF plants, Desalination 97 (1994) 171–187.
[25] A. Al-Radif, R. Borsani, H. Sultan, Selection of materials for Taweelah, ''B'' MSF desalination plant project (6×10–6×12.7 migd), Desalination 97 (1994) 3–16.
[26] K.S. Spiegler, A.D.K. Laird, Principles of deslaintion, 2nd ed., Academic Press, New York, 1980.
[27] A.M. Omar, Simulation of MSF desalination plants, Desalination 45 (1983) 65–67.
[28] A.M. Helal, M.S. Medani, M.A. Soliman, J.R. Flow, A tridiagonal matrix model for multistage flash desalination plants, Comput Chem. Eng. 10 (1986) 324–327.
[29] J.M. Montagna, N.J. Scennar, T. Melli, Some theoretical aspects in simulation of multi stage desalination systems, Proceedings of the Twelfth International Symposium on Desalination and Water Re-Use, Malta, 1991, pp. 437–448.
[30] A. Hussain, A. Hassan, D.M. Al-Gobaisi, A. Al-Radif, A. Woldai, C. Sommariva, Modelling, simulation, optimization, and control of multi-stage flashing (MSF) desalination plants. Part I: modelling and simulation, Desalination 92 (1993) 21–41.
[31] M. Rosso, A. Beltramini, M. Mazzotti, M. Morbidelli, Modeling multistage flash desalination plants, Desalination 108 (1996) 365–374.
[32] H.T. El-Dessouky, H.I. Shaban, H. Al-Ramadan, Multi-stage flash desalination process: a thermal analysis, Desalination 103 (1995) 271–287.
[33] H.T. El-Dessouky, S. Bingulac, A stage-by-stage algorithm for solving the steady state model of multi stage flash desalination plants, Desalination 107 (1996) 171–193.
[34] H.T. El-Dessouky, I. Alatiqi, H.M. Ettouney, Process synthesis: the multi-stage flash desalination system, Desalination 115 (1998) 155–179.
[35] H. El-Dessouky, H. Ettouney, Y. Al-Roumi, A novel multi-stage flash desalination brine circulation system, Ind. Eng. Chem. Res. (1998), submitted.
[36] K. Wangnick, K. Genthner, D.M.K.F. Al-Gobaisi, The next size generation of MSF evaporators: 100 000 m^3/d. II. Design and cost aspects, material selection, Proceedings of the IDA World Congress on Desalination and Water Sciences, Madrid, Spain, October 1997, vol. I, pp. 295324.
[37] H. El-Dessouky, I. Alatiqi, H. Ettonney, N. Deffeeri, Performance of wire mesh mist eliminators, Chem. Eng. Proc. (1998), submitted.